Geophysical Research Letters

RESEARCH LETTER
10.1029/2024GL111549

The Vertical Structure of Tropical Temperature Change in Global Storm-Resolving Model Simulations of Climate Change

Timothy M. Merlis[1], Ilai Guendelman[1], Kai-Yuan Cheng[1], Lucas Harris[2], Yan-Ting Chen[1], Christopher S. Bretherton[3], Maximilien Bolot[1], Linjiong Zhou[1], Alex Kaltenbaugh[2], Spencer K. Clark[2,3], and Stephan Fueglistaler[1]

[1]Program in Atmospheric and Oceanic Sciences, Princeton University, Princeton, NJ, USA, [2]Geophysical Fluid Dynamics Laboratory, NOAA, Princeton, NJ, USA, [3]Allen Institute for Artificial Intelligence, Seattle, WA, USA

Key Points:

- The vertical structure of tropical temperature change is assessed in global storm-resolving model (GSRM) simulations of climate change
- The GSRM analyzed, X-SHiELD, has a response to SST increase and CO_2 increase that are broadly similar to CMIP6 simulation results
- GSRM response to SST has muted warming through the mid-troposphere, but a large degree of amplification in the upper troposphere

Supporting Information:

Supporting Information may be found in the online version of this article.

Correspondence to:

T. M. Merlis,
tmerlis@princeton.edu

Citation:

Merlis, T. M., Guendelman, I., Cheng, K.-Y., Harris, L., Chen, Y.-T., Bretherton, C. S., et al. (2024). The vertical structure of tropical temperature change in global storm-resolving model simulations of climate change. *Geophysical Research Letters*, *51*, e2024GL111549. https://doi.org/10.1029/2024GL111549

Received 22 JUL 2024
Accepted 20 NOV 2024

Abstract Global storm-resolving model (GSRM) simulations (kilometer-scale horizontal resolution) of the atmosphere can capture the interaction between the scales of deep cumulus convection and the large-scale dynamics and thermodynamic properties of the atmosphere. Here, we assess the vertical structure of tropical temperature change in Geophysical Fluid Dynamics Laboratory's GSRM X-SHiELD, perturbed by a uniform sea surface temperature (SST) warming and/or increased CO_2 concentration. The simulated warming from an SST increase is weakly amplified relative to the surface through the mid-troposphere before increasing to a factor of about 2.5 in the upper troposphere. This combination of muted warming in the mid-troposphere and amplified warming aloft is within the range of CMIP6 models at individual pressure levels but, taken together, is distinctive behavior. The response to CO_2 increase with unchanged SST is an approximately vertically uniform warming, comparable to CMIP6 models, and is linearly additive with the SST-induced warming in X-SHiELD.

Plain Language Summary The vertical structure of tropical temperature change plays an important role in determining the magnitude of surface warming and modulates the strength of atmospheric convection and large-scale circulations in response to climate changes. How much enhancement of the tropical upper troposphere compared to the surface has been a longstanding question in climate science. Here, we assess this in climate timescale global storm-resolving model simulations of climate change with kilometer-scale horizontal resolution (3.25 km, roughly 20 times higher resolution than the atmospheric component of conventional climate models). Revisiting this question in this class of models is interesting because at kilometer-scale horizontal resolution, the atmospheric convection responsible for the enhanced heating—from the condensation of water vapor—of the upper troposphere is explicitly simulated. For the response to sea surface temperature warming, there is enhanced warming near the tropopause that is larger magnitude than typical climate models, while the middle of the troposphere (near 5 km altitude) has relatively muted warming compared to typical climate models. For the response to increased carbon dioxide concentration, this storm-resolving model has somewhat more tropospheric warming than typical climate models.

1. Introduction

Global storm-resolving models (GSRMs) of the atmosphere are a frontier of atmospheric modeling. To date, there are relatively few climate timescale simulations of the response of GSRMs to climate change. One climate response of long-standing importance that may have distinct behavior in this class of simulations is that of the tropical troposphere's temperature. Given the critical role of deep convection in setting the stratification of the tropical atmosphere and the GSRM explicit simulation thereof, this is an exciting area for comparison to conventional global climate models (GCMs) that parameterize deep convection. There is a long-standing question of how climate models compare to observed changes (e.g., Po-Chedley et al., 2021; Santer et al., 2005) and this is important to the global climate because it determines the clear-sky longwave radiative feedbacks (e.g., Feldl & Merlis, 2023; Held & Shell, 2012).

The starting point for understanding of the vertical structure of warming in the tropical troposphere is moist adiabats. Warmed moist adiabats have enhanced warming aloft relative to the surface as a result of increased latent heat release, a reduction in the temperature lapse rate (e.g., Hartmann, 2016). Undilute (i.e., non-entraining) moist adiabats have approximately a factor of 2.5 times as much warming in the upper troposphere as the surface.

Conventional GCMs typically have a factor of ≈2–2.5× more warming in the upper troposphere than at the surface. That they warm less than undilute moist adiabats is a long-standing result of GCM intercomparison (Santer et al., 2005), and this implies convective available potential energy (CAPE) increases with warming (e.g., Sobel & Camargo, 2011). There are several possible reasons for the sub-moist adiabatic warming. One of the key processes that is typically represented in cumulus parameterizations in GCMs is entrainment or dilution. In parcel theories with entrainment, neutrally buoyant entraining plumes can suppress upper tropospheric warming and capture changes in cloud-resolving model simulations of radiative convective equilibrium (Romps, 2016; Singh & O'Gorman, 2013). These theories have also been used to emulate the GCM response to climate change (Po-Chedley et al., 2019). The basic physical picture is that a constant entrainment rate leads to larger departures from an undilute profile with warming because the dilution increases with the saturation deficit. The saturation deficit $[q^*(1 - \mathcal{H})$, with saturation specific humidity q^* and relative humidity of the free troposphere $\mathcal{H}]$, in turn, has a Clausius-Clapeyron increase if the relative humidity changes are small. Beyond entrainment, there are radiative processes neglected in parcel theories such as the change in clear-sky radiative cooling profiles (which is bottom heavy for CO_2, Wang & Huang, 2019) and cloud radiative effects (all else equal an upward shift in high clouds will enhance the warming near the climatological cloud top, Li et al., 2019).

Aspects of the role that entrainment can play in the departure from moist adiabats with warming were developed in the idealized geometry of simulations of radiative convective equilibrium (Singh & O'Gorman, 2013; Wing & Singh, 2024). Here, we are examining comprehensive global simulations, with the divergent mean circulations at large scales. In response to warming, a deeper and weaker vertical velocity tends to reduce the adiabatic cooling in the mid-troposphere and modestly increase it near the tropopause (Figure 10 of Knutson & Manabe, 1995). Connecting entraining plume theory with weak temperature or pressure gradient theory for the vertical velocity produces warmer temperatures in the upper troposphere of ascending regions (Singh & Neogi, 2022). Nevertheless, the interaction with the mean circulation plays a secondary role for the tropical-mean temperature, so we simply compare the global models' simulated response to SST warming to moist adiabats and entraining plume theory with no representation of the divergent circulation.

GSRMs (also known as *k*-scale models for their kilometer-scale horizontal resolution) have emerged from a variety of numerical weather and climate model lineages and have been compared in 40-day long integrations in the DYAMOND intercomparison (Stevens et al., 2019). That intercomparison initialized from reanalysis to facilitate comparison to observations. There have also been GSRM simulations forced by perturbed SST and/or radiative forcing agents (e.g., Noda et al., 2019; Tsushima et al., 2014), though these have typically been somewhat coarser than the now prevalent ≈3 km horizontal resolution. The NICAM simulations presented in Tsushima et al. (2014) showed amplified warming in the tropical upper troposphere near 200 hPa that ranged from ≈2.5× the SST change (roughly in line with GCMs) to a factor of ≈4×, with sensitivity to the horizontal resolution (from 7 to 14 km), snow sedimentation rate, and a large sensitivity to the subgrid turbulence scheme (their Figure 11). Keil et al. (2023) showed that a perpetual-January simulation in 5 km ICON simulations forced with SST changes from an individual coupled GCM had warming in the tropical upper troposphere that was amplified by a factor between 2 and 2.5 relative to the surface. Here, we build off the X-SHiELD simulations first presented in Cheng et al. (2022) with 3.25 km horizontal resolution and assess the response of tropical mean temperatures to SST warming and/or increases in carbon dioxide concentration.

The X-SHiELD results are compared to the corresponding GCM simulations that took part in the Coupled Model Intercomparison Phase six (CMIP6). We compare their climatologies to reanalysis (Section 2). Then, we examine their response to uniform SST warming (Section 3.1) and the moist adiabatic response to determine whether these simulations fit within existing theories. We also examine their response to increased CO_2 with unchanged SST (Section 3.2) before concluding (Section 4).

2. Models and Methods

2.1. GSRM and GCMs

We analyze the 2-year long X-SHiELD simulations described in Bolot et al. (2023), Guendelman et al. (2024), and Merlis et al. (2024), among others. The atmosphere has 3.25 km horizontal resolution and 79 vertical levels. There is a shallow convection parameterization, but not one for deep convection. The land model is the Noah Land Surface Model, which has been used in National Centers for Environmental Prediction operational weather prediction (Ek et al., 2003). The simulation has a mixed layer ocean model with a 15-day relaxation timescale to

ECMWF analyzed SSTs from late October 2019 through the end of 2021. The 2-year period presented here is calendar years 2020 and 2021, meaning we discard more than 2 months as spinup period. The simulated X-SHiELD fields are coarsened online to 25 km and we subsequently interpolate to the standard CMIP6 pressure levels for all of the analysis here. Here, we present tropical means that are averages between 20° S and 20° N. There are four total 2-year long simulations: the control, one with uniform +4 K SST warming (unchanged CO_2 concentration), one with a CO_2 concentration increased to 1270 ppmv (unchanged SST, a 3.1 × CO_2 concentration perturbation), and a combined "global warming" perturbation simulation with both warmed SST and increased CO_2 concentration. The atypical CO_2 concentration change was an effort to have the global warming simulation close to the control simulation's global-mean top-of-atmosphere energy balance (Merlis et al., 2024), and we assume a logarithmic scaling in CO_2 concentration to present the results in terms of a 4 × CO_2 increase.

These GSRM simulations are compared to CMIP6 simulations using the amip, amip-p4K, and amip-4xCO_2 experiments (Eyring et al., 2016; Webb et al., 2017) averaged over the years 1980–2009. The 12 models are BCC-CSM2-MR, IPSL-CM6A-LR, MRI-ESM2-0, CESM2, GFDL-CM4, TaiESM1, CanESM5, CNRM-CM6-1, GISS-E2-1-G, HadGEM3-GC31-LL, MIROC6, and NorESM2-LM. These simulations are averaged over the period 1980–2009, and analogous figures for 2-year averages—to match the X-SHiELD integration length—are shown in Supporting Information S1. There is little sensitivity to the shorter averaging period.

2.2. Moist Adiabats

For the response to SST warming, we compare the vertical structure of the GSRM and GCM to moist adiabats (Section 3.1). The moist adiabats that we compare against for the SST warming perturbation are parcels lifted from 1000 hPa with the time- and zonal-mean tropical relative humidity and air temperature from the CMIP6 ensemble mean. We perturb the air temperature and surface relative humidity, though the latter has a modest effect. There is negligible sensitivity to calculating adiabats from the ensemble mean compared to averaging across adiabats from individual models. The lapse rate is a dry adiabat below the lifting condensation level, which is evaluated using the exact expression of Romps (2017). The rest of the sounding is obtained by numerically integrating the moist adiabatic lapse rate, using either the undilute moist pseudo adiabatic lapse rate (i.e., assuming condensed water is removed) or the theory of Romps (2016). This entraining plume theory (for the dilute adiabats) has a single non-dimensional parameter that is the entrainment rate scaled by the water vapor lapse rate. We set this to 0.2 and found that there are a range of values of comparable quality, none of which eliminate the structural issues with the model–dilute adiabat comparison (Section 3.1). We do not examine theories with additional parameters, such as Romps (2014) or Zhou and Xie (2019), which potentially can capture more detailed vertical structure at the expense of parsimony.

2.3. Control Climatology

Before we proceed to the response to SST warming and increased CO_2 concentration, we briefly examine the climatological tropical temperature distribution. This is shown in the skew-T log-p diagram in Figure 1a, with the 2-year mean of X-SHiELD in red, the ensemble mean of CMIP6 amip simulations in black, and the European Center for Medium-Range Weather Forecasts' ERA5 reanalysis (Hersbach et al., 2020) in magenta. Here, the reanalysis matches the years of the CMIP6 amip simulations. The tropical-mean soundings are comparable to moist adiabats: X-SHiELD and ERA5 largely overlap, while the CMIP6 ensemble-mean sounding more closely follows a colder moist adiabat. Because the X-SHiELD simulation period is later and samples two individual years, there can be a modest effect from the surface warming (linear trends are of order 0.1 K decade^{-1} in the tropics), but the individual years may also sample phases of the El Niño-Southern Oscillation or other internal variability that projects onto the free-troposphere's mean temperature (Fueglistaler, 2019; Sobel et al., 2002). Therefore, the model bias relative to ERA5 (Figure 1b) uses matched periods for a direct comparison: 2020 and 2021 for X-SHiELD and 1980–2009 for CMIP6.

Figure 1b shows that X-SHiELD, in general, has a smaller bias through much of the tropical troposphere compared to GCMs (≈ 1 K vs. ≈ 2 K from 500 hPa to 200 hPa), while it has a tropopause or cold point temperature that has a larger cold bias compared to GCMs (≈ 6 K vs. ≈ 2 K near 100 hPa). The GCM bias has intermodel spread that varies from ≈0.5 K in the lower troposphere to ≈1 K in the upper troposphere and X-SHiELD is typically within this envelope. The GCMs shown here all have cold biases in the upper

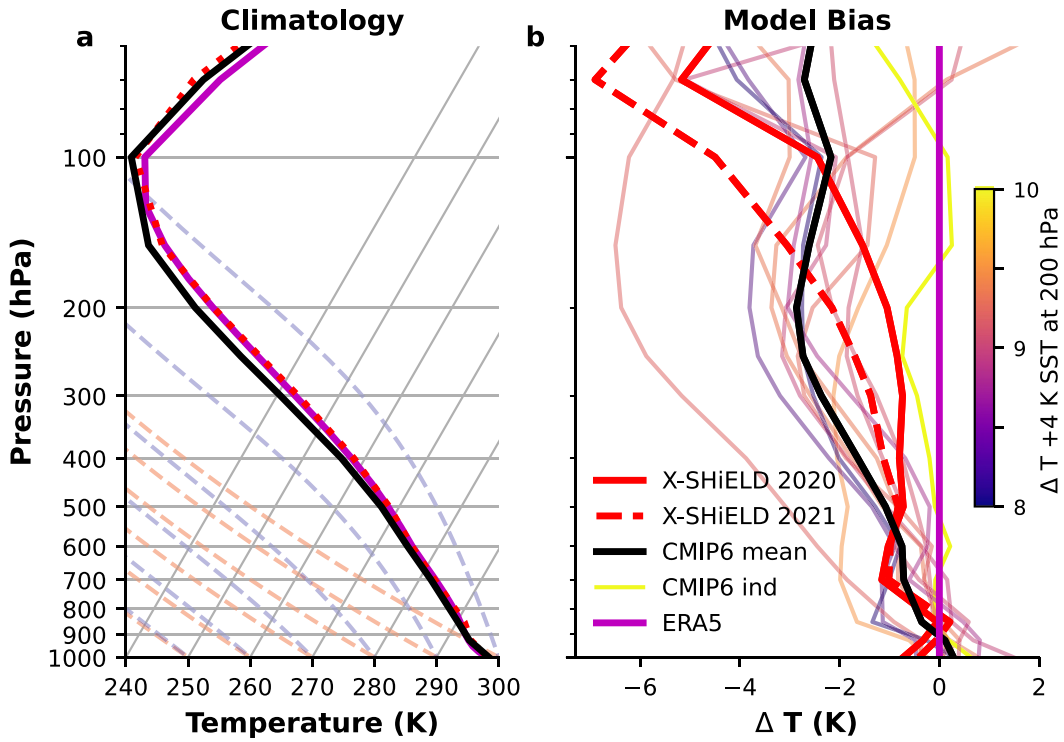

Figure 1. (a) Skew-T log-p diagram of the tropical-mean temperature of X-SHiELD (2-year mean in red dotted line), ERA5 (magenta line), and the ensemble-mean of CMIP6 models (black line) with dry adiabats shown in red dashed lines and moist adiabats shown in blue dashed lines and (b) model bias relative to ERA5 with the 2 years of X-SHiELD shown in red lines (with years indicated in legend), ERA5 in magenta, the ensemble-mean CMIP6 response shown in black line, and individual CMIP6 models in thin colored lines. The CMIP6 models are color-coded by the upper tropospheric (200 hPa) temperature response to SST warming, as shown by the colorbar. The time period used to calculate the bias relative to ERA5 differs between the CMIP6 models (time mean over 1980–2009, the years used for the CMIP6 climatology and shown in the skew-T plot) and X-SHiELD (annual means of the individual years indicated in the legend) to be consistent with the model simulation period analyzed.

troposphere, a known issue. However, we note that this set of GCMs is limited to the set of models that have performed the perturbation amip-p4K and amip-4xCO2 simulations.

There are, of course, a substantial number of additional control-climate, mean-state thermodynamic quantities that are of interest beyond temperature. Bao and Stevens (2021) presented several for the DYAMOND inter-comparison simulations. While this is an important aspect of model evaluation that may inform development, we turn to the response to SST warming and increased CO_2 concentration because of our interest in climate change.

3. Results

Figure 2 shows the response of X-SHiELD's tropical-mean atmospheric temperature to SST warming with unchanged CO_2 (a), CO_2 increase with unchanged SST (b), and the difference between the combined perturbation simulation and the sum of the two individual perturbation simulations (c), an examination of linearity. The response to SST warming is amplified in the upper troposphere, while the CO_2 warming is approximately vertically uniform. The combined perturbation simulation, which is closer to an energetically consistent global warming scenario as one would simulate with a coupled climate model, has a temperature response that is close to the linear superposition of the individual SST and CO_2 simulations through the troposphere (cyan line in Figure 2c is less than 0.1 K for pressures of 100 hPa or greater). We next provide a systematic comparison of X-SHiELD and CMIP6 simulations for the isolated SST warming and CO_2 increase.

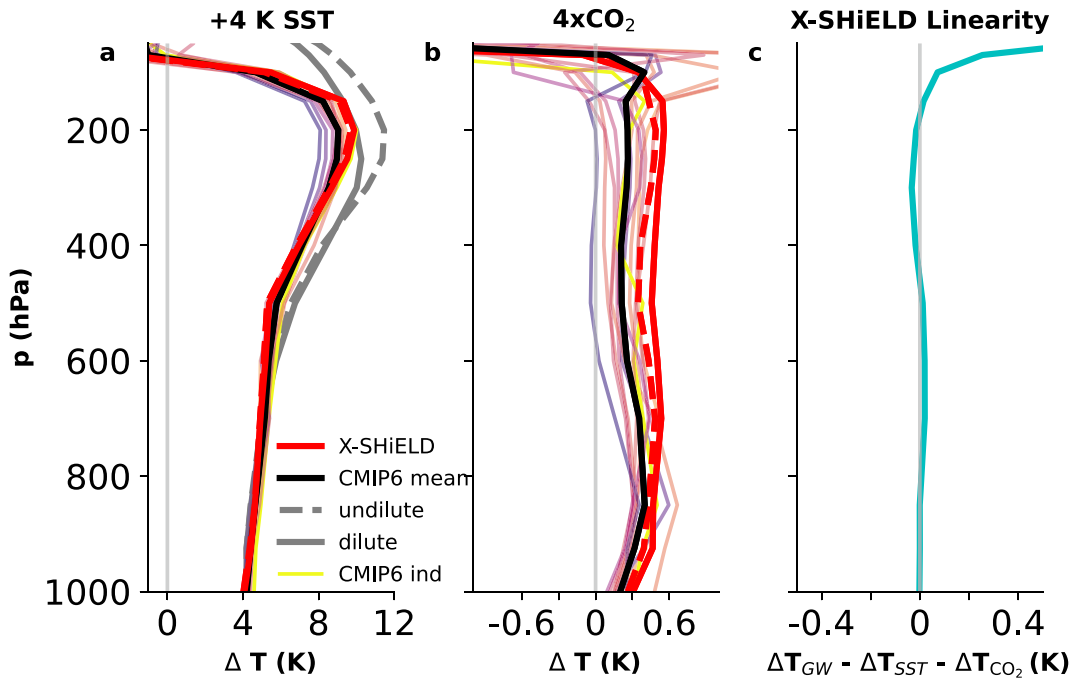

Figure 2. Profiles of the tropical mean temperature change in response to (a) +4 K of SST warming with unchanged CO_2 concentration, (b) 4× CO_2 concentration with unchanged SST, and (c) the difference between the combined global warming (GW) perturbation simulation in X-SHiELD and the sum of the two individual perturbation simulations (SST only and CO_2 only). The 2 years of X-SHiELD results are shown in red lines, undilute moist adiabat is shown in dashed gray line, dilute moist adiabat is shown in solid gray line, the ensemble-mean CMIP6 response is shown in black line, and individual CMIP6 models are shown in thin colored lines. The CMIP6 models are color-coded by the upper tropospheric (200 hPa) temperature response to SST warming for both panels (see colorbar in Figure 1b). Panel c is the average over both years, while the solid and dashed red lines in panels a and b show the mean of 2020 and 2021, respectively.

3.1. Response to SST Warming

The tropical temperature change increases with altitude in X-SHiELD and GCMs in response to a uniform +4 K SST increase (Figure 2a). The peak in the upper troposphere is nearly 10 K in X-SHiELD and occurs at 200 hPa (red lines). There are only modest ≈0.2 K differences in the temperature change between the 2 years of X-SHiELD in the troposphere. This peak warming is larger in magnitude than the CMIP6 ensemble-mean value of about 9 K (black line), though there is intermodel spread as the thin colored lines from individual GCMs indicates. Undilute moist adiabats have temperature changes that increase though the upper troposphere to ≈3 times the surface warming near 200 hPa (gray dashed line). This exceeds the GSRM and GCM response, with the latter previously documented in a number of studies (e.g., Miyawaki et al., 2020; Santer et al., 2005). The dilute moist adiabat shown here (solid gray line) has a warming maximum of about 10 K with its peak occurring at a higher pressure level (lower altitude) than the models (colored lines) or the undilute adiabat (gray dashed line). Keil et al. (2023) showed the GSRM ICON had upper troposphere amplified warming in a perpetual January simulation that was in the range of CMIP models (their Figure 2) for the SSP585 emissions scenario. (The direct responses to radiative forcing agents were not included in their GSRM, but were included in the CMIP6 simulations they compared with, though these are a modest percentage of the total.)

In addition to the upper tropospheric peak, we note that X-SHiELD has muted amplification of the surface warming to the mid-troposphere in comparison to CMIP6 GCMs (Figure 2a). There is 5.3 K of warming at 500 hPa, a mere 1.0 K or 23% more than the tropical-mean surface air temperature change. The ensemble mean of CMIP6 GCMs has an increase of 5.8 K at 500 hPa, a ≈35% amplification relative to the surface. As was the case for the upper troposphere, the adiabats are warmer than all models here too: 6.6 K and 6.4 K for the dilute and non-dilute adiabats, respectively.

In summary, all models (the GSRM and GCMs) have enhanced, but sub-adiabatic warming in the tropical upper troposphere. The GSRM X-SHiELD has warming that is muted through the mid-troposphere (up to about

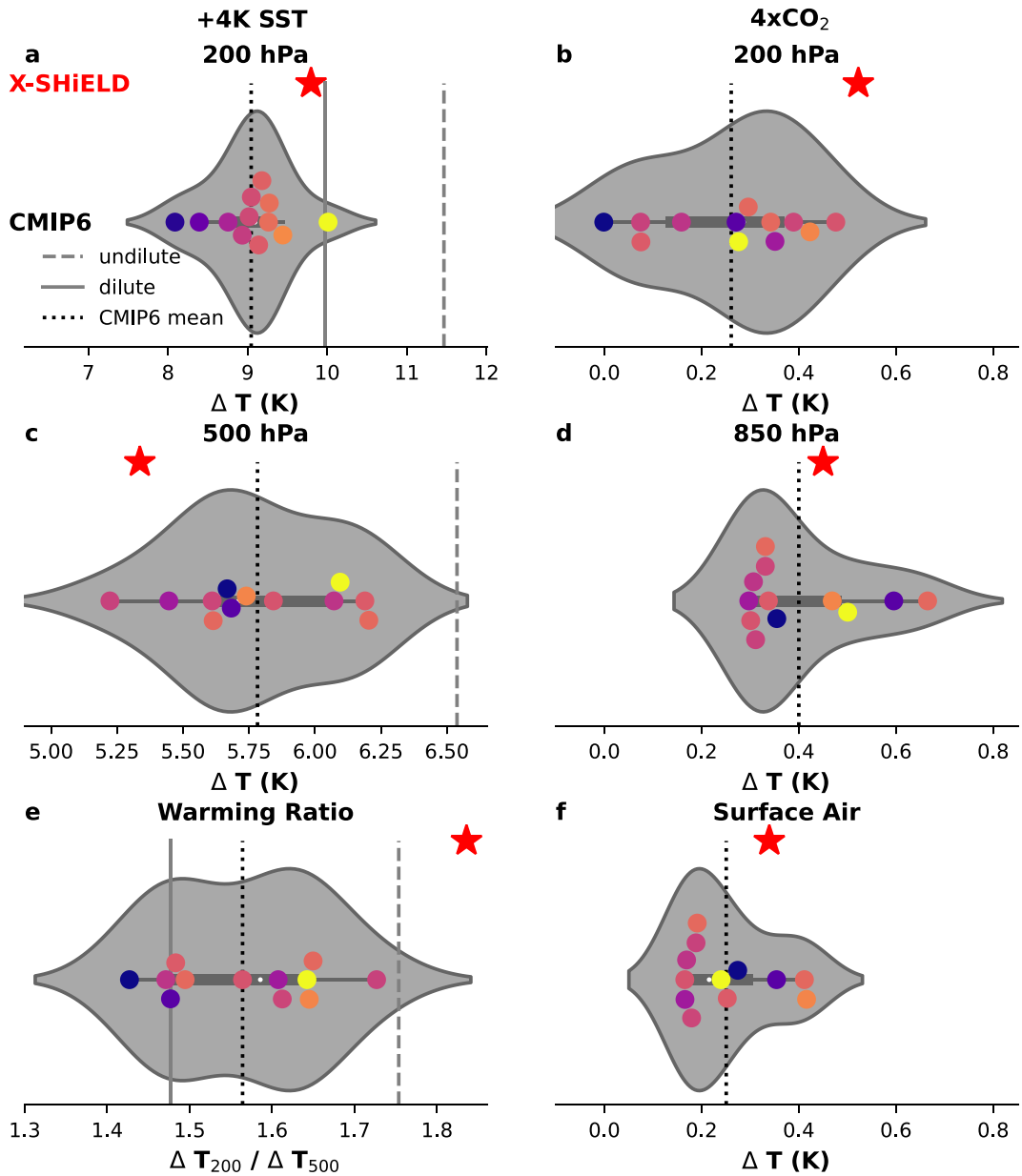

Figure 3. The tropical temperature response to (left) SST warming and (right) CO_2 increase at select levels. (a) Upper-troposphere (200 hPa) and (c) mid-troposphere (500 hPa) temperature response to SST warming for X-SHiELD (red star) and CMIP6 models (colored circles, with red indicating more upper-tropospheric warming in response to SST and blue indicating less upper-tropospheric warming) and their estimated distribution (gray violin) with the CMIP6 ensemble-mean shown in black dotted line, dilute adiabat in gray solid line, and undilute adiabat in gray dashed line. Note that the horizontal axis differs between panel a and c and is scaled such that ensemble-mean CMIP6 and undilute adiabat lines are at similar horizontal positions. (e) The warming ratio of the upper troposphere to the mid-troposphere from SST warming. (b) Upper-troposphere (200 hPa), (d) lower-troposphere (850 hPa), and (f) surface air temperature response to 4× CO_2 for X-SHiELD (red star) and CMIP6 models (colored circles with gray violin distribution). The color coding in all panels follows that of panel a, the upper troposphere temperature response to SST, to allow a visual assessment of whether the intermodel variation in response to SST warming and response to 4× CO_2 are related in these CMIP6 models.

500 hPa), but is warmer than the ensemble-mean of the GCMs in the upper troposphere. We next present a more detailed assessment of where X-SHiELD fits within the spread of the CMIP6 model ensemble.

Figure 3 shows the individual temperature responses of CMIP6 GCMs (colored circles) with the estimated distribution in gray lines at select vertical levels. Above this violin plot of the CMIP6 models, we have the 2-year

mean of the GSRM X-SHiELD shown in a red star. The X-SHiELD tropical upper troposphere temperature change of 9.8 K is larger than all but one individual CMIP6 model (Figure 3a). The CMIP6 models here and throughout are colored by this upper tropospheric response to SST warming, which allows us to compare the vertical coherence within the SST warming scenario (how tightly coupled are mid-tropospheric changes to those of the upper troposphere?) and to the climatology (does the control bias shown in Figure 1b constrain the response to warming?) and CO_2 forcing. In the mid troposphere, X-SHiELD is at the cold end of the CMIP6 distribution, with one of 12 GCMs having less warming (Figure 3c). The colors indicate that the warming at 500 hPa is correlated to 200 hPa, but weakly so with a coefficient of 0.40. These panels have different horizontal scales, but are designed to approximately match the ensemble-mean CMIP6 model in the middle (dotted line) and the undilute moist adiabat (dashed line) on the right. This illustrates that X-SHiELD warms more than the CMIP6 ensemble mean, but less than an undilute moist adiabat in the upper troposphere, as already noted in Figure 2. In the mid troposphere, X-SHiELD is below the CMIP6 ensemble mean, which is in turn below the undilute moist adiabat. Overall, X-SHiELD, were it a GCM in CMIP6, would be distinctive: relatively little warming through the mid troposphere and relatively high warming in the upper troposphere. This is clearly illustrated by the upper-to-mid troposphere warming ratio shown in Figure 3e. X-SHiELD has a ratio of ≈ 1.8, while the CMIP6 ensemble mean, extremal individual model, and undilute moist adiabat have warming ratios less than 1.75.

The physical reasons underlying X-SHiELD's distinctive vertical structure are unclear. The enhanced upper tropospheric warming is plausibly connected to X-SHiELD's increase in high clouds with warming (Bolot et al., 2023), which could give rise to locally enhanced radiative heating. However, our preliminary examination of the change in radiative heating rate suggests it is not a clear outlier compared to CMIP6 models. Additional research, including the potential role for sensitivities to model parameterizations (Abbott et al., 2024), is warranted.

3.2. Response to Increased CO_2

Increased CO_2 with unchanged SST modestly warms the troposphere by ≈ 0.3 K for a quadrupling of CO_2 in models, and there is little vertical structure to this warming (Figure 2b). The tropospheric warming is, to an extent, the result of interactive land surface temperatures. However, aquaplanet GCM simulations (Dinh & Fueglistaler, 2019; Merlis, 2015) and radiative convective equilibria (Romps, 2020) where the surface temperature is specified throughout the domain also have tropospheric warming as a direct response to CO_2 because the tropospheric temperature change is driven by decrease in tropospheric radiative cooling rate from increased CO_2. The overall sense from Figure 2b is that X-SHiELD has a similar vertical structure as the CMIP6 GCMs, but has a larger magnitude warming. This may be shaped, to an extent, by the transient nature of the short integration, as the second year of X-SHiELD has less warming (red dashed vs. red solid line in Figure 2b). Above the tropospheric warming, there is the well known stratospheric cooling that is an adjustment to the increased CO_2 concentration. X-SHiELD's stratospheric adjustment is broadly similar to CMIP6 GCMs, most of which is larger magnitude cooling than shown by the horizontal scale of Figure 2b. (There is somewhat more cooling in X-SHiELD for pressures lower than 10 hPa, not shown). This direct response of tropical temperature to increased CO_2 does not resemble moist adiabats, which has previously been documented (Miyawaki et al., 2020; Wang & Huang, 2019).

The X-SHiELD tropical upper-troposphere temperature adjustment to CO_2 of ≈ 0.5 K is larger than any individual CMIP6 model (Figure 3b). The CMIP6 models plotted here are colored by their upper tropospheric response to SST warming, and one can see that the intermodel spread in the response to SST does not simply govern the spread in the response to CO_2. Warm colors, which indicate a larger upper troposphere response to SST warming, are generally, but not exclusively, above the ensemble mean warming of 0.25 K for increased CO_2, and their correlation is not significant. It is plausible that the model spread may be the result of model-dependent and uncertain cloud adjustments. We have previously shown that X-SHiELD's adjustments to CO_2 includes an increase in tropical high clouds, which, all else equal, would warm the upper troposphere (Merlis et al., 2024).

In addition to the upper troposphere, we closely examine the model spread in the lower troposphere's temperature response to increased CO_2 at 850 hPa (Figure 3d). This is motivated by the CMIP6 ensemble-mean warming having a local maximum there (Figure 2b). The CMIP6 ensemble-mean warming of 0.4 K is the result of a large cluster of models with ≈ 0.3 K and a few with larger warming (Figure 3d). X-SHiELD has somewhat more warming at 850 hPa than the ensemble mean of CMIP6 (red star vs. black dotted line), but sits within the distribution (Figure 3d). The tropical surface air weakly warms in response to CO_2 with unchanged SST (Figure 3f).

The land's surface skin and air temperature can warm, but the surface air over the ocean can also modestly warm. This decreases the evaporative flux, helping to account for the decrease in precipitation that is a direct response to CO_2 increase. Dinh and Fueglistaler (2019) describe the coupling between the reduction in surface fluxes and vertical energy fluxes through the top of the boundary layer, as a mechanism for the enhanced warming there. The relatively enhanced warming at 850 hPa compared to the surface air (Figure 3f) is consistent with this, and it is robust across GCMs and X-SHiELD. The underlying physical origin of the weaker warming in the upper troposphere compared to the modestly bottom-heavy response to CO_2 in GCMs is an interesting question for additional research.

4. Conclusions

We have examined the vertical structure of atmospheric temperature change in the tropics in response to SST warming and CO_2 increase in 2-year simulations of a global storm-resolving model, Geophysical Fluid Dynamics Laboratory's X-SHiELD. This model's atmospheric temperature has a modest climatological bias compared to the ERA5 reanalysis, which is smaller than the bias of the multi-model mean of the CMIP6 models considered here (Figure 1b). For SST warming, the simulated temperature change is amplified aloft, with an upper tropospheric maximum that is about 2.5× the SST change. For CO_2 increase with unchanged SST, the simulated temperature change is a warming of about 0.5 K and is approximately vertically uniform in the troposphere. X-SHiELD's response to a combined SST and CO_2 perturbation is very similar to the linear sum of the two single perturbation simulations.

We compare these simulated GSRM temperature changes to CMIP6 GCM simulations and to moist adiabats. The warming structure is vertically amplified in all models, but to varying degrees and with differences in the pressure levels where the maximum enhancement occurs. All models, this GSRM and GCMs, have warming that is amplified, but by less than a moist adiabat. The GSRM is at the lower end of the range of GCMs for mid-tropospheric warming and at the upper end of the range of GCMs for the upper troposphere. This distinctive vertical structure of warming holds across the two simulated years when considered individually. This structure has limited impact on the temperature or lapse rate feedback (the change in top-of-atmosphere net radiation per unit surface warming) in the tropics compared to CMIP6 models: the more muted warming through the mid-troposphere makes the temperature feedback less stabilizing by ≈ 0.1 W m^{-2} K^{-1}, while the enhanced warming in the upper troposphere makes the temperature feedback more stabilizing by a comparable amount (using the zonal-mean of the radiative kernel of Pendergrass et al., 2018). The extent to which discrepancies between observed and GCM-simulated trends are altered in GSRM-simulated trends is an important question to address when longer integrations that include the patterned SST changes (vs. the uniform SST perturbation examined here) are feasible. We note that the available points of comparison are a 5 km horizontal resolution, perpetual-January ICON simulation, which has upper tropospheric amplification that is comparable to GCMs, and 7 to 14 km horizontal resolution NICAM simulations, with results that vary from comparable to GCMs to far warmer and outside the GCM range. This will be interesting to assess in other GSRMs as other long timescale SST warming simulations become available.

The response to CO_2 with unchanged SST (the tropospheric adjustment of temperature or the direct response of the tropospheric temperature to CO_2 forcing) is a warming of modest amplitude that is closer to vertically uniform than moist adiabatic. X-SHiELD has somewhat more warming than GCMs in the lower troposphere and is just outside the CMIP6 range in the upper troposphere. At present, there is no other GSRM available to compare against.

We presented the CMIP6 models color coded by the upper troposphere's response to SST and find weak correlations between this metric and the climatological upper troposphere's temperature (Figure 1) and between this metric and the response to CO_2 increase with unchanged SST (Figure 3).

It has been suggested that the response to SST warming of mesoscale organization of convection simulated in a GSRM affect precipitation extremes (Bao et al., 2024) and alter the stratification over cycles of internal variability in large-domain radiative convective equilibrium (Sokol et al., 2024). So, it is plausible that an increase in organization gives rise to the top-heavy vertical structure of temperature change seen here in response to SST warming. However, the I_{org} metric (Tompkins & Semie, 2017, calculated here using outgoing longwave radiation over the same tropical latitudes) has a nominal increase from 0.818 to 0.820 between the control and SST

warming simulations, which is small and likely not statistically significant. This does not rule out regional changes in convective organization behave in a manner that could influence the mean atmospheric temperature response to SST warming.

Additional research on both theory and GSRM configuration is warranted. Entraining plume theories are a useful point of comparison to these models (GCMs and GSRMs), as undilute moist adiabats warm more than all models in the upper troposphere. The single parameter class of dilute adiabat theory has vertical structure that differs from these models and this warrants additional work to identify parsimonious plume theories and objective procedures to determine their parameters. Detailing model sensitivities for the response to SST warming at kilometer-scale resolution is warranted. This includes radiative and microphysical sensitivities (e.g., Harrop & Hartmann, 2012; Tsushima et al., 2014). Finally, we note that the idealized uniform SST perturbation means that we cannot draw firm conclusions about the implications of this GSRM's upper tropospheric warming compared to observed trends.

Data Availability Statement

The source code of X-SHiELD is available at https://github.com/NOAA-GFDL/SHiELD_build. The CMIP6 simulation results are available from the Earth System Grid Federation at https://esgf-node.llnl.gov and the ERA5 reanalysis is available at Hersbach et al. (2023). The analysis code and data to reproduce these figures is provided in a zenodo archive at Merlis (2024).

Acknowledgments
We thank Camille Risi and Paul O'Gorman for perceptive feedback. The simulations presented in this paper were performed using High Performance Computing resources provided by the Cooperative Institute for Modeling the Earth System, with help from the Princeton Institute for Computational Science and Engineering. This study is supported under awards NA18OAR4320123, NA19OAR0220146, and NA19OAR0220147 from the National Oceanic and Atmospheric Administration (NOAA), U.S. Department of Commerce. This project is additionally funded by the NOAA Weather Program Office, Office of Oceanic and Atmospheric Research; and the NOAA Research Global-Nest Initiative. Bretherton and Clark acknowledge funding from the Allen Institute for Artificial Intelligence.

References

Abbott, T. H., Jeevanjee, N., Cheng, K.-Y., Zhou, L., & Harris, L. (2024). The land-ocean contrast in deep convective intensity in a global storm-resolving model. *Authorea Preprints*. https://doi.org/10.22541/essoar.172021737.79807737/v1

Bao, J., & Stevens, B. (2021). The elements of the thermodynamic structure of the tropical atmosphere. *Journal of the Meteorological Society of Japan. Ser. II*, *99*(6), 1483–1499. https://doi.org/10.2151/jmsj.2021-072

Bao, J., Stevens, B., Kluft, L., & Muller, C. (2024). Intensification of daily tropical precipitation extremes from more organized convection. *Science Advances*, *10*(8), eadj6801. https://doi.org/10.1126/sciadv.adj6801

Bolot, M., Harris, L., Cheng, K.-Y., Merlis, T. M., Blossey, P., Bretherton, C. S., et al. (2023). Kilometer-scale global warming simulations and active sensors reveal changes in tropical deep convection. *npj Climate and Atmospheric Science*, *6*(1), 209. https://doi.org/10.1038/s41612-023-00525-w

Cheng, K.-Y., Harris, L., Bretherton, C., Merlis, T. M., Bolot, M., Zhou, L., et al. (2022). Impact of warmer sea surface temperature on the global pattern of intense convection: Insights from a global storm resolving model. *Geophysical Research Letters*, *49*(16), e2022GL099796. https://doi.org/10.1029/2022gl099796

Dinh, T., & Fueglistaler, S. (2019). On the causal relationship between the moist diabatic circulation and cloud rapid adjustment to increasing CO_2. *Journal of Advances in Modeling Earth Systems*, *11*, 3836–3851. https://doi.org/10.1029/2019ms001853

Ek, M. B., Mitchell, K. E., Lin, Y., Rogers, E., Grunmann, P., Koren, V., et al. (2003). Implementation of Noah land surface model advances in the National Centers for Environmental Prediction operational mesoscale Eta model. *Journal of Geophysical Research*, *108*, D22. https://doi.org/10.1029/2002jd003296

Eyring, V., Bony, S., Meehl, G. A., Senior, C. A., Stevens, B., Stouffer, R. J., & Taylor, K. E. (2016). Overview of the coupled model intercomparison project phase 6 (CMIP6) experimental design and organization. *Geoscientific Model Development*, *9*(5), 1937–1958. https://doi.org/10.5194/gmd-9-1937-2016

Feldl, N., & Merlis, T. M. (2023). A semi-analytical model for water vapor, temperature, and surface-albedo feedbacks in comprehensive climate models. *Geophysical Research Letters*, *50*(21), e2023GL105796. https://doi.org/10.1029/2023gl105796

Fueglistaler, S. (2019). Observational evidence for two modes of coupling between sea surface temperatures, tropospheric temperature profile, and shortwave cloud radiative effect in the tropics. *Geophysical Research Letters*, *46*(16), 9890–9898. https://doi.org/10.1029/2019gl083990

Guendelman, I., Merlis, T. M., Cheng, K.-Y., Harris, L., Bretherton, C. S., Bolot, M., et al. (2024). The precipitation response to warming and CO_2 increase: A comparison of a global storm resolving model and CMIP6 models. *Geophysical Research Letters*, *51*(7), e2023GL107008. https://doi.org/10.1029/2023gl107008

Harrop, B. E., & Hartmann, D. (2012). Testing the role of radiation in determining tropical cloud top temperature. *Journal of Climate*, *25*(17), 5731–5747. https://doi.org/10.1175/jcli-d-11-00445.1

Hartmann, D. (2016). *Global physical climatology*. Elsevier.

Held, I. M., & Shell, K. M. (2012). Using relative humidity as a state variable in climate feedback analysis. *Journal of Climate*, *25*(8), 2578–2582. https://doi.org/10.1175/jcli-d-11-00721.1

Hersbach, H., Bell, B., Berrisford, P., Hirahara, S., Horányi, A., Muñoz-Sabater, J., et al. (2023). ERA5 monthly averaged data on single levels from 1940 to present [Dataset]. *Copernicus Climate Change Service (C3S) Climate Data Store (CDS)*. https://doi.org/10.24381/cds.f17050d7

Hersbach, H., Bell, B., Berrisford, P., Hirahara, S., Horányi, A., Muñoz-Sabater, J., et al. (2020). The ERA5 global reanalysis. *Quart. J. Roy. Meteor. Soc.*, *146*(730), 1999–2049. https://doi.org/10.1002/qj.3803

Keil, P., Schmidt, H., Stevens, B., Byrne, M. P., Segura, H., & Putrasahan, D. (2023). Tropical tropospheric warming pattern explained by shifts in convective heating in the Matsuno–Gill model. *Quart. J. Roy. Meteor. Soc.*, *149*(756), 2678–2695. https://doi.org/10.1002/qj.4526

Knutson, T. R., & Manabe, S. (1995). Time-mean response over the tropical Pacific to increased CO_2 in a coupled ocean-atmosphere model. *Journal of Climate*, *8*(9), 2181–2199. https://doi.org/10.1175/1520-0442(1995)008<2181:tmrott>2.0.co;2

Li, Y., Thompson, D. W. J., Bony, S., & Merlis, T. M. (2019). Thermodynamic control on the poleward shift of the extratropical jet in climate change simulations: The role of rising high clouds and their radiative effects. *Journal of Climate*, *32*(3), 917–934. https://doi.org/10.1175/jcli-d-18-0417.1

Merlis, T. M. (2015). Direct weakening of tropical circulations from masked CO_2 radiative forcing. *Proceedings of the National Academy of Sciences*, *112*(43), 13167–13171. https://doi.org/10.1073/pnas.1508268112

Merlis, T. M. (2024). Supporting data for "The vertical structure of tropical temperature change in global storm-resolving model simulations of climate change". *Collections*. https://doi.org/10.5281/zenodo.12785771

Merlis, T. M., Cheng, K.-Y., Guendelman, I., Harris, L., Bretherton, C. S., Bolot, M., et al. (2024). Climate sensitivity and relative humidity changes in global storm-resolving model simulations of climate change. *Science Advances*, *10*(26), eadn5217. https://doi.org/10.1126/sciadv.adn5217

Miyawaki, O., Tan, Z., Shaw, T. A., & Jansen, M. F. (2020). Quantifying key mechanisms that contribute to the deviation of the tropical warming profile from a moist adiabat. *Geophysical Research Letters*, *47*(20), e2020GL089136. https://doi.org/10.1029/2020gl089136

Noda, A. T., Kodama, C., Yamada, Y., Satoh, M., Ogura, T., & Ohno, T. (2019). Responses of clouds and large-scale circulation to global warming evaluated from multidecadal simulations using a global nonhydrostatic model. *Journal of Advances in Modeling Earth Systems*, *11*(9), 2980–2995. https://doi.org/10.1029/2019ms001658

Pendergrass, A. G., Conley, A., & Vitt, F. M. (2018). Surface and top-of-atmosphere radiative feedback kernels for CESM-CAM5. *Earth System Science Data*, *10*(1), 317–324. https://doi.org/10.5194/essd-10-317-2018

Po-Chedley, S., Santer, B. D., Fueglistaler, S., Zelinka, M. D., Cameron-Smith, P. J., Painter, J. F., & Fu, Q. (2021). Natural variability contributes to model–satellite differences in tropical tropospheric warming. *Proceedings of the National Academy of Sciences*, *118*(13), e2020962118. https://doi.org/10.1073/pnas.2020962118

Po-Chedley, S., Zelinka, M. D., Jeevanjee, N., Thorsen, T. J., & Santer, B. D. (2019). Climatology explains intermodel spread in tropical upper tropospheric cloud and relative humidity response to greenhouse warming. *Geophysical Research Letters*, *46*(22), 13399–13409. https://doi.org/10.1029/2019gl084786

Romps, D. M. (2014). An analytical model for tropical relative humidity. *Journal of Climate*, *27*(19), 7432–7449. https://doi.org/10.1175/jcli-d-14-00255.1

Romps, D. M. (2016). Clausius-Clapeyron scaling of CAPE from analytical solutions to RCE. *Journal of the Atmospheric Sciences*, *73*(9), 3719–3737. https://doi.org/10.1175/jas-d-15-0327.1

Romps, D. M. (2017). Exact expression for the lifting condensation level. *Journal of the Atmospheric Sciences*, *74*(12), 3891–3900. https://doi.org/10.1175/jas-d-17-0102.1

Romps, D. M. (2020). Climate sensitivity and the direct effect of carbon dioxide in a limited-area cloud-resolving model. *Journal of Climate*, *33*(9), 3413–3429. https://doi.org/10.1175/jcli-d-19-0682.1

Santer, B. D., Wigley, T. M. L., Mears, C., Wentz, F. J., Klein, S. A., Seidel, D. J., et al. (2005). Amplification of surface temperature trends and variability in the tropical atmosphere. *Science*, *309*(5740), 1551–1556. https://doi.org/10.1126/science.1114867

Singh, M. S., & Neogi, S. (2022). On the interaction between moist convection and large-scale ascent in the tropics. *Journal of Climate*, *35*(14), 4417–4435. https://doi.org/10.1175/jcli-d-21-0717.1

Singh, M. S., & O'Gorman, P. A. (2013). Influence of entrainment on the thermal stratification in simulations of radiative-convective equilibrium. *Geophysical Research Letters*, *40*(16), 4398–4403. https://doi.org/10.1002/grl.50796

Sobel, A. H., & Camargo, S. J. (2011). Projected future seasonal changes in tropical summer climate. *Journal of Climate*, *24*(2), 473–487. https://doi.org/10.1175/2010jcli3748.1

Sobel, A. H., Held, I. M., & Bretherton, C. S. (2002). The ENSO signal in tropical tropospheric temperature. *Journal of Climate*, *15*(18), 2702–2706. https://doi.org/10.1175/1520-0442(2002)015<2702:tesitt>2.0.co;2

Sokol, A. B., Munteanu, V. A., Blossey, P. N., & Hartmann, D. L. (2024). Internal ocean-atmosphere variability in kilometer-scale radiative-convective equilibrium. *ESS Open Archive*. https://doi.org/10.22541/essoar.172202788.81317674/v1

Stevens, B., Satoh, M., Auger, L., Biercamp, J., Bretherton, C. S., Chen, X., et al. (2019). DYAMOND: The DYnamics of the atmospheric general circulation modeled on non-hydrostatic domains. *Progress in Earth and Planetary Science*, *6*, 1–17. https://doi.org/10.1186/s40645-019-0304-z

Tompkins, A. M., & Semie, A. G. (2017). Organization of tropical convection in low vertical wind shears: Role of updraft entrainment. *Journal of Advances in Modeling Earth Systems*, *9*(2), 1046–1068. https://doi.org/10.1002/2016ms000802

Tsushima, Y., Iga, S., Tomita, H., Satoh, M., Noda, A. T., & Webb, M. J. (2014). High cloud increase in a perturbed SST experiment with a global nonhydrostatic model including explicit convective processes. *Journal of Advances in Modeling Earth Systems*, *6*(3), 571–585. https://doi.org/10.1002/2013ms000301

Wang, Y., & Huang, Y. (2019). Understanding the atmospheric temperature adjustment to CO_2 perturbation at the process level. *Journal of Climate*, *33*(3), 787–803. https://doi.org/10.1175/jcli-d-19-0032.1

Webb, M. J., Andrews, T., Bodas-Salcedo, A., Bony, S., Bretherton, C. S., Chadwick, R., et al. (2017). The cloud feedback model intercomparison project (CFMIP) contribution to CMIP6. *Geoscientific Model Development*, *10*(1), 359–384. https://doi.org/10.5194/gmd-10-359-2017

Wing, A. A., & Singh, M. S. (2024). Control of stability and relative humidity in the radiative-convective equilibrium model intercomparison project. *Journal of Advances in Modeling Earth Systems*, *16*(1), e2023MS003914. https://doi.org/10.1029/2023ms003914

Zhou, W., & Xie, S.-P. (2019). A conceptual spectral plume model for understanding tropical temperature profile and convective updraft velocities. *Journal of the Atmospheric Sciences*, *76*(9), 2801–2814. https://doi.org/10.1175/jas-d-18-0330.1